Briefings in Bioinformatics, 18(5), 2017, 837–850

doi: 10.1093/bib/bbw061
Advance Access Publication Date: 25 July 2016
Paper

Comparative assessment of differential network analysis methods

Yvonne Lichtblau, Karin Zimmermann, Berit Haldemann, Dido Lenze, Michael Hummel and Ulf Leser

Corresponding author: Knowledge Management in Bioinformatics, Institute for Computer Science, Humboldt-Universität zu Berlin, Unter den Linden 6, 10099 Berlin, Germany. Tel: +49 30 2093 3904; Fax: +49 30 2093 5484; E-mail: yvonne.lichtblau@informatik.hu-berlin.de

Abstract

Differential network analysis (DiNA) denotes a recent class of network-based Bioinformatics algorithms which focus on the differences in network topologies between two states of a cell, such as healthy and disease, to identify key players in the discriminating biological processes. In contrast to conventional differential analysis, DiNA identifies changes in the interplay between molecules, rather than changes in single molecules. This ability is especially important in cases where effectors are changed, e.g. mutated, but their expression is not. A number of different DiNA approaches have been proposed, yet a comparative assessment of their performance in different settings is still lacking. In this paper, we evaluate 10 different DiNA algorithms regarding their ability to recover genetic key players from transcriptome data. We construct high-quality regulatory networks and enrich them with co-expression data from four different types of cancer. Next, we assess the results of applying DiNA algorithms on these data sets using a gold standard list (GSL). We find that local DiNA algorithms are generally superior to global algorithms, and that all DiNA algorithms outperform conventional differential expression analysis. We also assess the ability of DiNA methods to exploit additional knowledge in the underlying cellular networks. To this end, we enrich the cancer-type specific networks with known regulatory miRNAs and compare the algorithms performance in networks with and without miRNA. We find that including miRNAs consistently and considerably improves the performance of almost all tested algorithms. Our results underline the advantages of comprehensive cell models for the analysis of -omics data.

Key words: differential network analysis; gene-regulatory networks; miRNAs; transcriptome data; biomarker

Introduction

Each cell in the body harbors a vast amount of different biochemical entities, most of which interact with many other entities to perform diverse functions [1]. Network models allow us to represent, investigate and visualize such interactions at large scale. Studying these networks quantitatively and qualitatively is a core topic of Systems Biology [2–4]. Recently, a novel approach to network analysis, called differential network

Yvonne Lichtblau finished her Master in Bioinformatics in 2013 and currently works as a PhD student in network-based biomarker detection in the group of Prof. Leser, Humboldt-Universität zu Berlin, Germany.
Karin Zimmermann has finished her Master in Bioinformatics in 2008 and is now working as a PhD student in Bioinformatics approaches to the study of differential splicing in Lymphoma in the group of Prof. Leser, Humboldt-Universität zu Berlin, Germany.
Berit Haldemann has finished her Diploma in Bioinformatics in 2010 and since works as a Bioinformatician in the statistical analysis of different types of -omics data.
Dido Lenze is working as a biology Postdoc in the Institute of Pathology at Charité – Universitätsmedizin Berlin.
Michael Hummel is the research group leader of the Institute of Pathology at Charité – Universitätsmedizin Berlin. His general topic of research is molecular mechanisms in malignant lymphomas and the main current research interest is the epigenetic gene regulation of Hodgkin lymphoma.
Ulf Leser holds the Chair of Knowledge Management in Bioinformaticcs at the department for Computer Science of Humboldt-Universität zu Berlin, Germany. His main topics of research are biomedical text mining, statistical analysis of -omics data sets and scalable workflows for the analysis of next-generation sequencing data.
Submitted: 2 March 2016; **Received (in revised form):** 3 June 2016

analysis (DiNA), was proposed, which measures the change in network structure (topology and edge weights/activation strength) between two different states of the same cellular network, such as healthy versus cancerous or wild-type versus mutated [5–7]. DiNA builds on two successful lines of prior work: (1) differential expression analysis (DEA), focusing on the difference in abundance of a single entity or groups of entities between two states, such as the expression levels of genes [8–11], and (2) network expression analysis (NEA), which studies the role of single entities within a given network, such as the centrality of genes in a disease network [12–17]. By combining these two ideas, DiNA overcomes their respective limitations: compared with DEA, DiNA takes the complexity of many phenotypical changes into account which cannot be tracked down to the changes of single entities. In contrast to NEA, it focuses on the changes within the underlying network which more directly hints to key players associated to or even causing these changes. DiNA algorithms are particularly suitable for cases in which phenotypical changes are caused by rewiring in the network, due to changes in gene regulatory relationships [5,18–20], for instance, or when key players are changed but their expression is not, such as a mutation in a transcription factor (TF) influencing its function but not its own regulation [5,21–23]. Several recent works have demonstrated the potential of this approach: in [24–26], the authors performed DiNA on gene expression correlation networks and identified key transcriptional regulators involved in cancer, even though their expression levels were not changed significantly. Fuller et al. [23] discovered body-weight-related genes using DiNA on networks of two mouse strains. Hudson et al. [22] compared gene co-expression networks constructed from two different breeds of bulls, one with and one without a known mutation in the TF myostatin. Although myostatin was not differentially expressed, DiNA ranked it highest when comparing the networks. The common theme of DiNA algorithms is the comparison of two states of the same underlying network (Figure 6). Most often, gene co-expression networks are used, i.e. networks in which nodes represent genes or proteins, and edges are determined using co-expression analysis based on microarrays or RNASeq data. DiNA algorithms first compute a score for each gene in each network and subsequently rank genes based on the difference in their scores. In contrast to conventional DEA, these scores reflect properties of the network topology. For instance, genes could first be scored by their degree in a co-expression network, i.e. the number of other genes whose expression values are significantly correlated, and then ranked by the degree change, thus identifying genes whose connectivity in the networks changes the most [5,27].

Several sophisticated variations of this general scheme have been proposed, such as DiffK [23], DCGlob/DCLoc [21] or DiffRank [28]. They differ, for instance, in the degree to which they consider global network changes for gene scores (node degree is a particularly simple and local measure) and the way how differences in the gene score are computed. However, it is currently unclear whether any of these methods is generally better in identifying entities altered in a given disease than the others, as no comparative assessment has been performed, yet. Furthermore, we are not aware of any study which assesses DiNA methods on different types of networks. Gene co-expression networks are popular, but must be considered as a largely incomplete model for a cell, as a multitude of different regulatory players is ignored. One important class of such molecules is MicroRNAs (miRNA), which are stretches of RNA that act as negative post-transcriptional regulators of gene expression by binding to partially complementary sites of mRNAs. Thereby, they cause inhibition of translation or, in most cases, degradation of the mRNAs [29]. In human, around 1200 different miRNA are known, playing a role in the regulation of more than 30% of all known mRNAs [30]. MicroRNA de-regulation is associated with the development and the progression of various diseases [31]. In particular, they are believed to act as tumor suppressors and oncogenes in different cancer types [32].

In this work, we compare the relative performance of 10 DiNA algorithms on co-expression networks using gold standard gene lists. Our analysis is built on a recently published high-quality human regulatory network containing only experimentally verified interactions from public databases and expert curated text-mining [33]. For four types of cancer (prostate adenocarcinoma (PRAD), breast invasive carcinoma (BRCA), lung adenocarcinoma (LUAD) and liver hepatocellular carcinoma (LIHC)), we constructed four instances of this network to compare healthy and cancerous samples with and without miRNAs. Each pair of healthy/disease networks was analyzed by the 10 different DiNA algorithms with the goal to recover genes that are known to play an important role in the respective cancer. We find that results of DiNA methods clearly cluster by their general underlying strategy, that local DiNA methods are overall superior to global methods, that all DiNA methods outperform conventional differential expression analysis and that the inclusion of miRNAs consistently and considerably improves the performance of almost each tested method. By performing extensive randomization experiments, we show that these positive effects also remain when the changes in network topology introduced by the often highly connected miRNA are removed, which indicates that the inclusion of miRNA co-expression brings truly new knowledge into the networks which can be exploited by most DiNA methods. Our results underline the advantages of comprehensive cell models for the analysis of -omics data.

Results

Cancer-specific human regulatory networks

To compare the performance of DiNA algorithms on regulatory networks, we used a recently published high-quality human regulatory core network of TFs and the genes they regulate which was created using public databases and expert-curated text mining [33]. Henceforth, this network is called gene regulatory network (GRN). To assess the influence of miRNAs on the performance of DiNA algorithms for regulatory networks, we augmented this network with all known miRNAs and their regulatory relationships to form the so-called miRNA–enhanced GRN*. Figure 1 shows the sources of every kind of regulatory interaction in these networks. Altogether we extracted 13 550 regulatory interactions among 517 TFs, 510 miRNAs and 3739 genes and TFs. As all data either stems from manually curated databases, from expert-curated text mining, or from multiple, independent data sources, we consider both networks to be of high quality.

These two core networks were transformed into cancer-type specific networks by weighting edges with gene expression correlation scores from cancer-type-specific experiments and their respective controls. Edges with non-significant correlation values were removed, see section Methods. This procedure was performed for four different types of cancer: PRAD, BRCA, LIHC and LUAD. Eventually, we obtained 16 different networks: GRN* and GRN for each cancer-type and tissue-specific control.

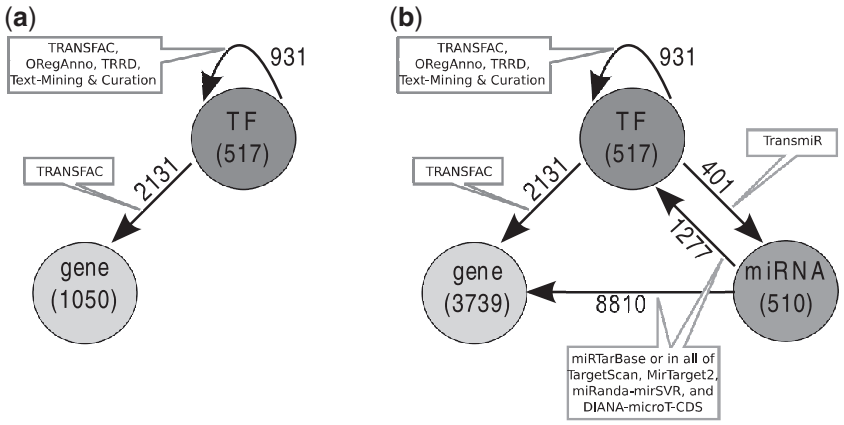

Figure 1. Structure and sources of the core regulatory network. (A) The gene regulatory network (GRN) comprises only genes and TFs with their regulatory relationships. (B) The miRNA–enhanced gene regulatory network (GRN*) adds miRNAs and their relationships. Numbers denote the count of each type of regulatory interaction and the text fields specify their origin.

Table 1. Number of entities, relationships and selected network characteristics of the gene regulatory networks (GRN*) and of the miRNA–enhanced gene regulatory networks (GRNs*) for the prostate adenocarcinoma data set (PRAD) after applying the correlation cutoff (see section Methods). Values consider only the largest connected component, which here contains 94% (disease GRN*), 98% (control GRN*), 93% (disease GRN) and 95% (control GRN) of all edges. asp, average shortest path length

	Disease GRN*	Control GRN*	Disease GRN	Control GRN
#TF →TF	121	171	115	167
#TF →gene	502	601	489	589
#TF →miRNA	40	81	0	0
#miRNA →TF	161	257	0	0
#miRNA →gene	832	1531	0	0
#edges	1656	2641	604	756
#TFs	264	323	163	216
#miRNAs	118	146	0	0
#genes	922	1334	352	432
#nodes	1304	1803	515	648
Average degree TFs	3.8	4.2	4.8	4.7
Average degree genes	1.5	1.7	1.4	1.4
Average degree mirnas	8.8	12.8	–	–
#triangles	35	49	31	30
diameter	14	12	10	14
asp	5.8	5.3	4.6	5.1

Generally, the GRN*s have nearly three times as many edges and nodes as the GRNs. Table 1 shows the important network characteristics for all four networks of the PRAD data set. Although the number of edges and nodes highly differs between GRNs and GRNs*, all four networks are highly similar in many structural aspects such as average shortest path (min: 4.6, max: 5.8), diameter (min: 10, max: 14), average degree of TFs (min: 3.8, max: 4.8), average degree of genes (min: 1.4, max: 1.7) and the distribution of degrees (Supplementary Figure S7.2).

MicroRNAs have a considerably higher degree (8.8 in the disease GRN* and 12.8 in the control GRN* for PRAD) than TFs. This is consistent with the literature, as single miRNAs may have dozens or even more targets [30]. Genes have the lowest average degree, as they are not regulating other entities. Note that the number of TF →TF and TF →Gene edges differs between GRNs and GRNs* because miRNAs add new connecting edges into the network, which can prevent the removal of other edges from the connected component of a network. Our observations made on the GRNs and GRNs* for PRAD are consistent for the other data sets (Supplementary Table S7.1).

Selection of DiNA algorithms and evaluation procedure

The purpose of our study is to compare the performance of DiNA algorithms and to assess the impact of miRNAs on the performance of DiNA algorithms in finding disease-associated genes using transcriptome data. To obtain a robust finding, we perform this analysis not with a single DiNA algorithm, but instead selected 10 different algorithms, most of which were recently published: DiffK [23], DCLoc and DCGlob [21], DiffRank [28], local structure (LS) measure [28], differential degree/betweenness/PageRank/Eigenvector centrality (DDC, DBC, DPC and DEC) [13,28,34,35] and differential motif centrality (DMC) [34,36]. A detailed description of each algorithm can be found in the Methods section. The 10 considered algorithms can be classified into three groups. The first group (*global*) measures global changes in the topology of the networks (DBC, DPC, DEC and DCGlob). For instance, DPC computes the DPC of each node in each network and ranks nodes based on the change in their DPC. The second group (*local*) focuses on local changes (DDC, DMC, DiffK, LS and DCLoc); as an example, DiffK computes the sum of edge weights of each node with all its neighbors and ranks nodes based on the changes in this sum. The third group (*hybrid*) comprises only the method DiffRank which uses a combination of local and global measures. We used a gold standard list (GSL_V) for each cancer type to assess the performance of the algorithms. We derived this list from a general cancer-census list published by Vogelstein et al. [37] which we augmented with cancer-specific miRNAs. As a primary quality indicator, we computed the overlap between top-k results of the considered algorithms and the respective GSLs for each cancer type. We chose $k = 40$ which is supported by the graphical display of the distribution of differential centrality scores, see Supplementary Figure S7.3 and Methods section).

Relative performance of DiNA algorithms

Table 2 shows the mean number of recovered key components within the 40 top-ranked nodes over all cancer data sets for the

Table 2. Average number of recovered key components from GSL_V in the miRNA–enhanced gene regulatory networks (GRNs*) over all cancer data sets for each class of DiNA algorithm (local/global/hybrid)

DiNA algorithm class	Mean number of recovered entities
Local (DiffK, DDC, LS, DCLoc and DMC)	11.5
Global (DBC, DPC, DCGlob and DEC)	7.3
Hybrid (DiffRank)	14.3

different classes of DiNA algorithms (local/global/hybrid). With a value of 14.3, the hybrid DiffRank (partly based on betweenness centrality) recovers the most entities (genes, TFs and miRNAs) on an average for GSL_V. For the other two classes, algorithms considering local changes in topology recover, on an average, three entities more from GSL_V than the algorithms considering global topology changes. The improvement is particularly clear in the case of the DCLoc/DCGlob pair of algorithms; DCLoc achieves considerably better results than DCGlob (Table 3), although both are based on the same principles, but one uses only local changes and one only global changes.

DBC achieves the best results of the global topology algorithms. On an average, it finds 12.5 entities from GSL_V compared with the overall average of the global DiNA algorithms of 7.3 nodes (Table 3). Notably, DBC, like DiffRank, is based on betweenness centrality, which, in contrast to other common centrality measures, may also assign nodes a high rank that are not well connected locally [35]. Another interesting case is DMC, which explicitly takes the motifs each node is part of into account (feed-forward loops). Since miRNAs often co-regulate the expression of targets together with TFs in such loops [27,38,39], it is highly expected that DMC improves with the inclusion of miRNAs and so it does (compare upper and lower parts of Table 3). DCGlob depends on significantly differential edge weights between the disease and the control network. Recovery rates are very low for LUAD and LIHC, which is due to the very small result lists DCGlob produces. This method works only well when the data set is large and shows only good results in the PRAD and BRCA data sets. DPC does not work well on any data set; likely because it can only find nodes which are regulated by other nodes (incoming edges) as central but not nodes which regulate many other nodes (outgoing edges). Results obtained on cancer-type specific GSLs from MalaCards [40] confirm our results (see section Methods and Supplementary S7.4).

DiNA algorithms cluster on their algorithmic basis

We compare different DiNA algorithms based on the concrete entities they recover. To this end, we count how many common nodes (genes, TFs and miRNAs) are detected by pairs of two different methods and cluster all methods according to the Jaccard index across all data sets (Figure 2).

The clustering generally resembles the classification of the algorithms in global, local and hybrid, but there are also outliers. The lower cluster in Figure 2 contains three local, one global (DBC) and the one hybrid method and encompasses the best algorithms in our evaluation; within this cluster, DBC and DiffRank, both based on betweenness centrality, form an own subcluster. The rooting of DBC in the degree-independent betweenness centrality score gives this method an advantage over the other methods. The upper cluster contains three global (DPC, DEC and DCGlob) and two local methods (DCLoc and DMC). DMC and DCLoc produce few miRNAs in their results, which is in contrast to the other local approaches (Supplementary Table S7.8).

Performance of DiNA compared to conventional differential expression

We also compared the performance of DiNA methods with two baselines: (1) conventional differential expression analysis (DEA) of single genes [10], and (2) minimum redundancy–maximum relevance (MRMR) [41], which improves on DEA by considering statistical dependencies between genes. Results are shown in Table 4. MRMR produces significantly enriched result lists in three out of four cases and thus performs much better than DEA, but still largely inferior to most DiNA algorithms. Strikingly, results of MRMR contain only miRNA among the top-40 entities, meaning that this method filtered away all relevant TFs and genes.

DiNA results significantly improve with miRNA

Extending on the results listed in Table 3, we compared the ability of 10 DiNA algorithms to recover key players in four different cancer types in the GRNs*, consisting of genes, TFs and miRNAs, with that in the GRNs, consisting only of genes and TFs for different k. Results are plotted in Figure 3 and associated P values assessing the significance of the overlap sizes are shown in Table 3. Note that our method to derive P values takes the different set sizes of the GSLs and the different network sizes into account. The most striking observation is that recovery rates improve drastically for almost all 10 algorithms in all four cancer types when moving from GRN to GRN*.

The absolute number of detected nodes from GSL_V improves in 35 out of 40 cases, but remains unchanged for DPC in PRAD, DEC in LUAD and DCGlob in LIHC. In many cases, recovery rates nearly double. Taking DiffRank as an example, we see improvements from 4 to 17 recovered genes, TFs or miRNAs in BRCA, from 6 to 10 in PRAD, from 6 to 17 in LIHC and from 8 to 13 in lung cancer. The P values obtained in GRNs* are significant (P value $<=0.05$) in 33 out of 40 cases, whereas P values in GRNs are mostly not significant. Figure 4A shows a heatmap visualizing the differences in the number of recovered key components.

One difference when comparing the GSLs between the GRN* and the GRN is that the former contains miRNAs, whereas the latter does not. Accordingly, the improvements in recovery rates could be due only to many miRNAs showing up in the top-k results. To assess this possibility, we perform the same evaluation as before, but this time only consider genes and TFs in the GSLs. Figure 4B proves that improvements are still visible. Recovery rates improve in 58% of the cases (maximum improvement: three entities) and degrade in 25% of the cases (maximum deterioration: four entities). The total numbers of entities across all combinations that are recovered in the GRN* are much higher than the total number of entities recovered only in the GRN, meaning that miRNAs have a positive impact on DiNA algorithms even if only their regulated genes are focused. This is confirmed by the resulting P values (Supplementary Table S7.5).

Table 3. The upper table shows the number of detected nodes and enrichment *P* values from GSL_V in the top-40 results of each DiNA algorithm when using the miRNA–enhanced gene regulatory network (GRN*). The bottom table gives the same information when applying the DiNA methods to the gene regulatory networks (GRNs). PRAD, prostate adenocarcinoma; BRCA, breast invasive carcinoma; LIHC, liver hepatocellular carcinoma; LUAD, lung adenocarcinoma

Method	PRAD		BRCA		LUAD		LIHC	
	Number	*P* value	Number	*P* value	Number	*P* value	Number	*P* value
	GRNs*							
DBC	13	3.8e−08	12	3.4e−07	13	1.8e−07	12	5.6e−06
DMC	9	0.00014	8	0.00075	5	0.088	11	3.6e−05
DPC	5	0.054	7	0.0036	5	0.088	4	0.34
LS	11	3e−06	19	5e−15	13	1.8e−07	14	9.9e−08
DiffRank	10	2.2e−05	17	1.5e−12	13	1.8e−07	17	9.9e−11
DiffK	14	3.5e−09	16	2.2e−11	11	1.1e−05	14	9.9e−08
DDC	11	3e−06	16	2.2e−11	7	0.0083	11	3.6e−05
DCLoc	6	0.016	12	3.4e−07	11	1.1e−05	10	2e−04
DCGlob	9	0.00014	7	0.0036	2	1	2	1
DEC	5	0.054	5	0.051	4	0.3	12	5.6e−06
	GRNs							
DBC	10	0.00011	7	0.0056	7	0.015	8	0.0031
DMC	6	0.04	5	0.07	3	0.75	6	0.043
DPC	5	0.18	5	0.07	6	0.05	3	0.74
LS	7	0.012	6	0.022	7	0.015	7	0.013
DiffRank	6	0.04	4	0.28	8	0.0037	6	0.043
DiffK	9	0.00062	7	0.0056	8	0.0037	7	0.013
DDC	9	0.00062	7	0.0056	9	0.00075	6	0.043
DCLoc	4	0.33	4	0.28	5	0.18	9	0.00066
DCGlob	3	0.74	6	0.022	1	0.34	2	1
DEC	4	0.33	3	0.49	4	0.51	2	1

Discussion

Impact of the distribution of correlation values

The distribution of Spearman's correlation values in the different networks could be the source for two different kinds of bias in our results. First, differences in the distribution of correlations between the networks for cancerous and control tissue could result in deviating rankings of the entities leading to incorrectly derived differential centralities. Second, differences in the distribution of correlations between edges adjacent to miRNAs and edges not adjacent to miRNAs could be a bias when comparing results obtained with GRNs* and GRNs. Therefore, we inspect the distribution of correlations in our networks (Supplementary Table S7.6). Correlations in all networks are normally distributed (Wilk–Shapiro test) with mean 0. The standard deviation ranges from 0.20 to 0.32, but is similar between control and cancerous tissue given a cancer data set. The last column of Supplementary Table S7.6 gives the percent of absolute correlations greater than the theoretical significance threshold given the sample size. Only edges with a significant correlation will be used for the final networks. For all data sets, there are more significant correlations in the normal tissue network than in the cancer tissue network, as also observed in [42]. Supplementary Figure S7.7 shows the distribution of correlation values for each kind of interaction of the BRCA regulatory network (top) and the corresponding regulatory network derived from the normal tissue (bottom). For regulatory interactions between TFs and genes or other TFs, there are clearly more positive significant correlation values. For regulatory interactions by miRNAs, more negative edges are significant. This meets expectations since miRNAs are negative regulators of gene expression [29]. Nevertheless, not all regulatory interactions by miRNAs are negative because negative feedback circuits can result in an overall positive regulation as reported in [43,44]. In summary, we do not find a strong bias in our results due to changes in the distribution of correlation values.

Correlation of DiNA results and node degree

All interactions of the types TF →miRNA, TF →TF and TF →gene are derived from experimental analysis of individual genes. Genes and TFs from GSL_V that are known to play an important role in the development of cancer have a bias towards higher network degrees because these genes were investigated more frequently. To test if these nodes are recovered more easily by DiNA algorithms, we retrieved the top-40 entities for each DiNA algorithm and calculate the Spearman correlation between each entitie's degree in a network and its differential score. Supplementary Table S7.8 lists the top-20 entities according to each DiNA algorithm exemplarily for the PRAD data set. Notably, LS, DiffK and DDC rank more miRNAs than other algorithms; here 18–20 out of the 20 top-ranked nodes are miRNAs. MicroRNAs also have the highest average degree in our networks (Table 1). Supplementary Table S7.9 shows that indeed for three local DiNA algorithms, the correlation between node degree and differential score is significant (>0.31) in the control network. For LS, the averaged correlation over all data sets is 0.79 for the control networks and 0.49 for the disease networks, for DiffK, it is 0.61 and 0.17, respectively, and for DDC, 0.4 and 0.17, respectively. This is expected as the differential score directly depends on the number of edges or the sum of edge weights. For the global DiNA algorithms, DEC, DiffRank and DBC, the correlation between degree and differential score is significant only in the control networks. For DBC, the

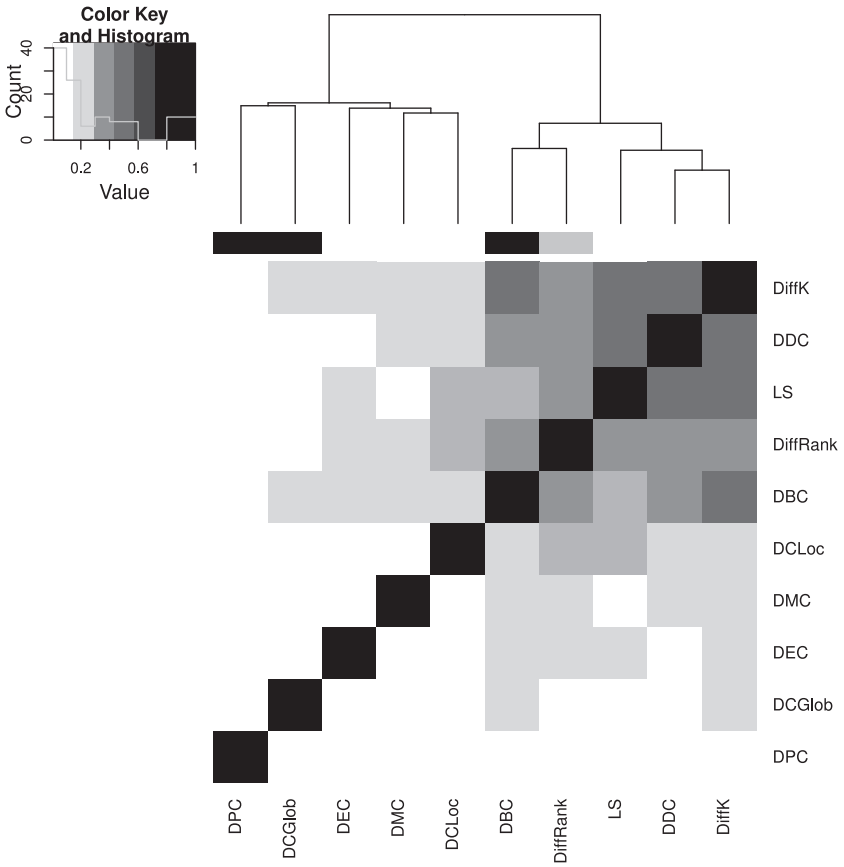

Figure 2. Clustering of DiNA algorithms according to the Jaccard Index across all data sets. The colors denote the class of the DiNA algorithm. Black: global DiNA algorithms (DBC, DCGlob, DPC and DEC), White: local DiNA algorithms (DiffK, DDC, LS, DCLoc and DMC), Grey: hybrid DiNA algorithm (DiffRank).

Table 4. Enrichment of gold standard list (GSL_{V}) with significantly differentially expressed genes, TFs and miRNAs. PRAD, prostate adenocarcinoma; BRCA, breast invasive carcinoma; LIHC, liver hepatocellular carcinoma; LUAD, lung adenocarcinoma; DEA, differential expression analysis; MRMR, minimum redundancy–maximum relevance

	DEA		MRMR	
	Number	*P* value	Number	*P* value
PRAD	1	1	3	0.15
BRCA	1	1	15	9.2e−12
LUAD	0	0.4	13	6.3e−10
LIHC	1	1	9	3.4e−05

correlation is 0.41 and 0.28, respectively. It also gives nodes a high rank although they have a low degree but play an important role in the larger topology, e.g. bridges, in the respective cancer network. In summary, for some DiNA algorithms, there is a significant correlation, hinting to their vulnerability to a publication bias.

Effect of network structure

An important difference between GRNs* and GRNs that influences DiNA results is their variety in size and topologies. To study the impact of these factors, we create two types of randomized networks. In the first type, called edge-shuffled, we shuffle the miRNA targets randomly. In the second type, called randomly weighted, we distort the GRN* by assigning random edge weights sampled from a normal distribution with mean and standard deviation equal to that of the true correlation values. We then compare DiNA results for both types of randomized networks with that of the original GRNs* using $GSL_{V,}$ expecting the difference between the original network and the randomly weighted networks to be smaller than that between the original network and its edge-shuffled counterparts, as still the same entities are connected by regulatory links. Figure 5A visualizes the relative performance of the original and the edge-shuffled networks. As expected, results are much better for the non-randomized network (on an average 4.1 more entities); differences are particularly high for DiffRank, DCLoc, DBC and LS. And as expected, the difference in recovery rates is higher between the original networks and the edge-shuffled networks than between the original networks and the randomly weighted networks (Figure 5B). This shows that DiNA methods in general are very sensitive to the topology of the underlying networks.

To further test the impact of edge weights and network topology, we computed the intersections of the DiNA algorithm's results across the four different cancer types. If the underlying, experimentally obtained expression values had only a small influence on the results, each DiNA algorithm should produce similar rankings regardless of the particular cancer type. This clearly is not the case, as can be seen in Table 5 and Supplementary Figure S7.10.

For LS, we have the largest intersection: 11 nodes are among the top-40 nodes of each cancer type, eight of which are

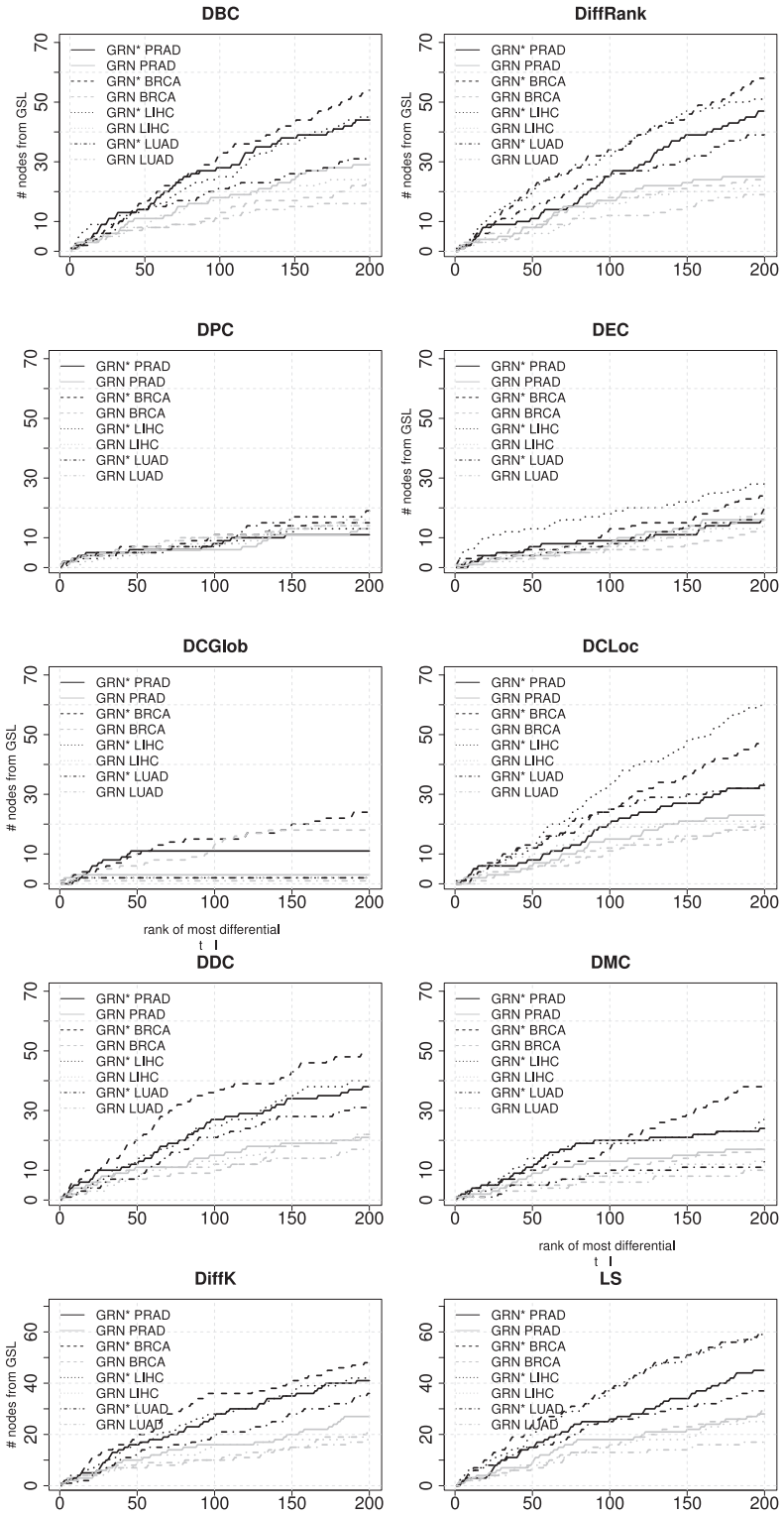

Figure 3. Overlaps of top-k results of 10 DiNA algorithms with the GSL_V lists for each cancer type for k=1–200 (x-axis). Black solid and dashed lines depict overlap sizes in the miRNA–enhanced gene regulatory network (GRNs*), grey solid and dashed lines in the gene regulatory networks (GRNs). PRAD, prostate adenocarcinoma; BRCA, breast invasive carcinoma; LIHC, liver hepatocellular carcinoma; and LIHC, lung adenocarcinoma.

miRNAs. For DiffRank, the intersection contains eight nodes (four miRNAs). Intersections of the other methods are of no relevance, i.e. zero to 5 nodes. The small sizes of the intersections emphasize the strong impact of the individual experimental evidences on the outcome of the DiNA algorithm. In summary, these results show that the topology of the underlying regulatory network plays a critical role in DiNA and underline the importance of using high-quality networks to cope with the high levels of noise typically observed in transcriptome data [45–47]. Including miRNAs notably changes this

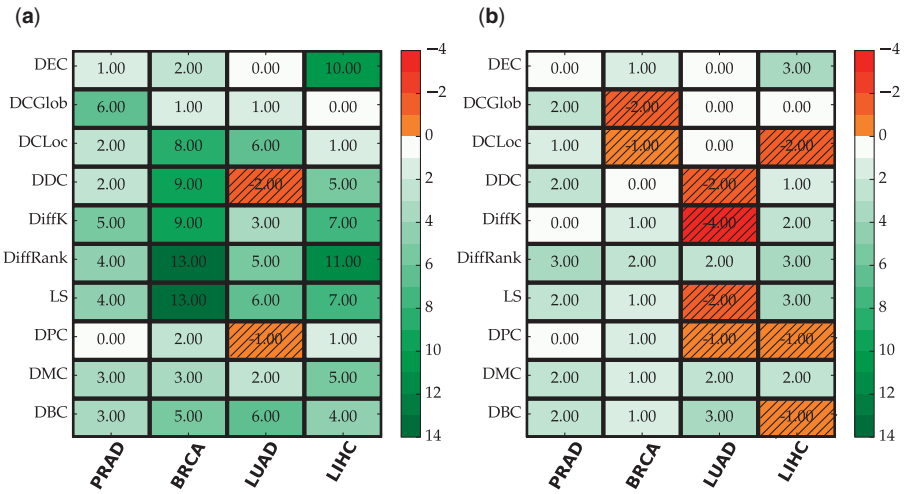

Figure 4. Heatmaps of the improvements in the number of recovered key components from GSL_V when using the miRNA-enhanced gene regulatory network (GRN*) instead of the gene regulatory network (GRN). (A) Number of genes, TFs or miRNAs from GSL_V contained in the top-40 results of DiNA algorithms. (B) The number of genes and TFs from GSL_V contained in the top-40 results of DiNA algorithms after removing miRNAs from the rankings. Unshaded cells represent cases where more elements from the GSL are recovered with the GRN* than with the GRN. Shaded cells represent cases where less GSL elements were recovered. Brightness of colors indicates the number of improved/degraded key components (see legend). PRAD, prostate adenocarcinoma; BRCA, breast invasive carcinoma; LIHC, liver hepatocellular carcinoma; LUAD, lung adenocarcinoma. A colour version of this figure is available at BIB online: https://academic.oup.com/bib.

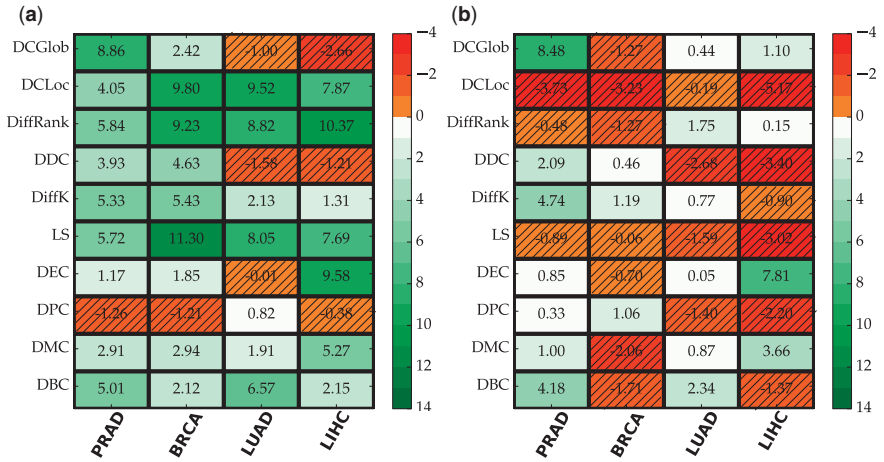

Figure 5. Difference in the number of identified entities from GSL_V between the results obtained with the original miRNA–enhanced gene regulatory networks (GRNs*) and the randomized networks. Difference to (A) the mean of 100 edge-shuffled networks and (B) the mean of 100 randomly weighted networks. Unshaded cells represent cases where the results with the GRNs* are better than with the randomized networks. Shaded cells represent cases where the results obtained with the GRNs* are worse than with the ranodmized networks. Brightness of colors indicates the number of improved/degraded key components (see legend). PRAD, prostate adenocarcinoma; BRCA, breast invasive carcinoma; LIHC, liver hepatocellular carcinoma; LUAD, lung adenocarcinoma. A colour version of this figure is available at BIB online: https://academic.oup.com/bib.

Table 5. Common genes, TFS and miRNAs found by the DiNA algorithms among the top-40 for all four cancer data sets

Rank	Intersection #genes, TFs	#miRNAs
DBC	1	1
LS	3	8
DDC	1	4
DiffRank	4	4
DPC	2	0
DCLOC	3	1
DCGLOB	1	0
DiffK	1	3
DMC	4	0
DEC	0	0

Table 6. Size and composition of gold standard list GSL_V for each type of cancer. PRAD, prostate adenocarcinoma; BRCA, breast invasive carcinoma; LIHC, liver hepatocellular carcinoma; LUAD, lung adenocarcinoma

Cancer	**Genes, TFs**	miRNAs	$\sum$
PRAD	84	27	111
BRCA	88	57	145
LUAD	59	30	89
LIHC	76	58	134

topology; however, their positive effects on DiNA performance are not only due to these changes but also heavily depend on the concrete experimental data brought into the analysis (Table 5).

Influence of correlation cutoff on the results

To test how strongly the results depend on the chosen correlation cutoff, we repeat the experiments for the PRAD data set with two further cutoffs. We compare the results obtained with our original cutoff of 0.33 to the results obtained with a 10% lower cutoff of 0.3 and with a 10% higher cutoff of 0.36. Results are shown in Supplementary Table S7.11. For each DiNA algorithm, we calculate the intersection of nodes from GSL_V ranked among the top-40 in each of the three settings for the correlation cutoff. Looking at DBC, we find 13 nodes from GSL_V with the original cutoff, 14 for the lower cutoff and 13 for the higher cutoff. For all DiNA algorithms, the differences are at most one node. While the number of nodes identified from GSL_V hardly changes, it is important to carefully choose the cutoff. We determine the cutoff by using a statistical test (see section Methods).

Conclusion

In this work, we compare the performance of 10 DiNA algorithms on four cancer transcriptome data sets for networks without miRNA to those on networks including miRNA. When comparing these algorithms to each other, local methods and, even more, one hybrid algorithm outperforms methods considering global network changes. All DiNA methods outperform conventional differential expression analysis. Several studies have shown that considering miRNAs improves performance in single network analysis [27,39,48,49]; however, their impact on DiNA has not been studied before. Evaluated on two sets of gold standard gene lists, we find that consideration of miRNA almost always considerably improves recovery rates. Improvements are due partly to a better ranking of genes and TFs and partly to correctly identified miRNA. We based our evaluation mostly on the cancer gene list from [37] (GSL_V). Note that genes and TFs from this list are unspecific with respect to the cancer types. However, this does not imply that all genes in this list are equally relevant for all types of cancer; instead, it should be considered as a union of several cancer-type-specific lists. Accordingly, it is not surprising that our analysis produces different gene lists depending on the cancer type which the underlying transcriptome data were obtained from. Obviously, the best evaluation would be based on cancer-type-specific GSLs; however, we are not aware of such lists with robust community acceptance. Our findings cannot directly be extrapolated to other configurations of DiNA. DiNA is based on the underlying network, which in this work is a rather small, high-quality regulatory core network obtained by manual curation of published findings. DiNA algorithms rank only the entities contained in its network, which is here enriched for TFs [33]. Therefore, performance of DiNA could be different on pure correlation networks or on protein–protein interaction networks [21–23,25,26,28]. Nevertheless, our results are a strong evidence for (a) the strength of DiNA algorithms to find key players in regulatory networks based on transcriptome data and (b) the advantages of using more comprehensive regulatory models than those just building on genes.

Materials and methods

In this section, we first give an overview of our workflow (Figure 6), then we describe each step in detail. Initially, we selected RNASeq data sets from The Cancer Genome Atlas [50] for four different cancerous and corresponding normal tissues. Next, we mapped pairwise correlation values on gene levels into cancer-specific edge weights in two high-quality human core regulatory networks obtained from public databases and literature curation. We used two such networks. In the miRNA–GRNs*, genes, TFs and miRNAs are contained. In the GRNs, only genes and TFs are represented. For each cancer type, four networks were created: GRN* for cancerous tissue, GRN* for control tissue, GRN for cancerous tissue and GRN for control tissue. We analyzed each pair of networks using 10 DiNA algorithms and evaluated each method by its ability to identify those genes which are known to play an important role in the respective cancer using GSLs. Data processing was generally performed using the statistical programming environment *R* [51]. For network construction, network analysis, calculation of differential centralities in the disease networks and the comparison of the networks, we use *Python* [52] and the *NetworkX* package [53].

RNASeq data sets and processing

We downloaded mRNASeq and miRNASeq data sets from four different cancer types available from TCGA [50]: prostate adenocarcinoma (ID: PRAD), breast invasive carcinoma (ID: BRCA), lung adenocarcinoma (ID: LUAD) and liver hepatocellular carcinoma (ID: LIHC). We used preprocessed TCGA data sets (Level 3), i.e. count values for each miRNA were already aggregated/calculated. Data were quality checked and normalized using the *DESeq* package [10]. In each data set, we only used those samples where cancerous and control tissues stem from the same patients, leading to 36 expression sets for PRAD, 83 for BRCA, 40 for LIHC and 17 for LUAD. We downloaded all data sets in January 2014.

Assembling a human regulatory core network

Analysis was performed on the basis of the same underlying human regulatory core network. The miRNA–GRNs* consist of miRNA, genes and TFs and their regulatory interactions represented as directed edges: miRNA → gene, miRNA → TF, TF → gene, TF → miRNA and TF → TF. In contrast, the GRNs only consist of genes and TFs and their relationships to each other. They are generated by simply removing all miRNA and adjacent edges from the GRN*. The GRN* was constructed based on a carefully selected set of data sources (Figure 1A). (1) Relationships between miRNA and other entities were taken from the database miRTarBase [54] which only contains experimentally validated relationships. Additionally, we extracted miRNA-target relationships listed in all four of the databases TargetScan [55], MirTarget2 [56], miRanda-mirSVR [57] and DIANA-microT-CDS [58]; since these databases contain only computationally predicted targets, we follow the suggestion of [59] and require a relationship to be predicted in all of them before accepting it for our network. For all these databases, we used the versions available as of June 2015; our selection of miRNA prediction tools follows the suggestions of [60]. (2) Relationships between TFs and genes or other TFs were obtained from TRANSFAC [61], ORegAnno [62] and TRRD [63], all of which are curated databases. We augmented these data with an additional set of 865 TF–TF relationship from an in-house curation project. This set is generated by first identifying potential TF–TF relationship using automated text mining in all PubMed abstracts, followed by manual curation of the top-2500 sentences where curators explicitly took the strength of the experimental evidence reported in the respective paper into account; the method is described in detail in [33]. (3) Regulations of miRNA by TFs were taken from TransmiR [64] which contains

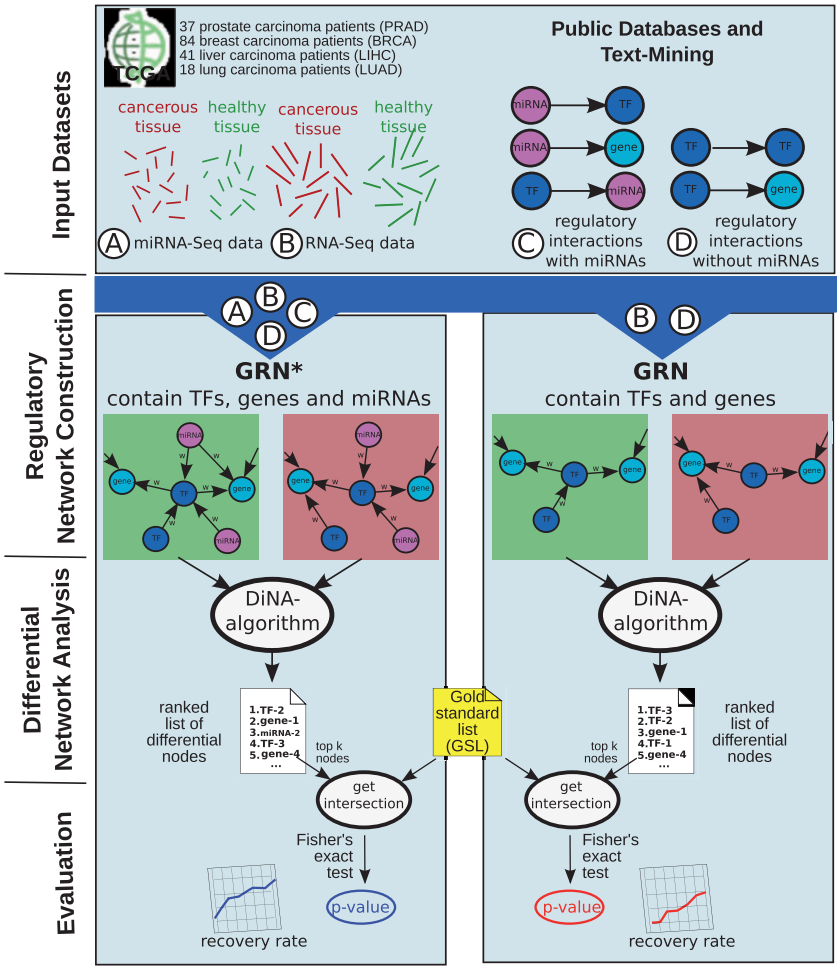

Figure 6. Workflow of our approach. A colour version of this figure is available at BIB online: https://academic.oup.com/bib.

only manually curated human regulatory relationships. TFs and genes were mapped to their corresponding HGNC symbol [65]. In summary, all interactions of the types TF →miRNA, TF →TF and TF →gene are derived from experimental analysis of individual genes. Of the miRNA →TF and miRNA →gene interactions, 30% are experimentally verified, whereas the remaining 70% are predicted. Note that all the regulatory interactions we use are not tissue specific (we are not aware of tissue specific regulatory networks). We partly address this problem by removing edges with non-significant correlation values (see next Section), as only nodes with a significant correlation value are supposed to interact with each other [5].

Cancer-specific networks with/out miRNA

The core networks GRN and GRN* are transformed into cancer-specific weighted networks by assigning each edge a initial weight corresponding to the correlation strength of expression values of the adjacent nodes in the respective RNAseq data set. Correlation is computed using Spearman's rank correlation which does not make assumptions about the distribution of the underlying data [66,67]. Signs of relationships are determined from the sign of correlation between the two genes. For some DiNA algorithms, the edge weights are transformed (see next section). To obtain the final networks, we applied a significance threshold to remove edges with non-significant correlation values: we tested if the correlations are significantly different from zero (P value < 0.05) by using the t-distribution. A requirement for this test is the normality of the correlation values which we ensured beforehand by applying the Shapiro–Wilk test [68]: for each network, we randomly draw 100 values from all correlations and calculated the P value. This was repeated 100 times and the mean P value is calculated for each network. Only for calculating DCGlob and DCLoc, no threshold was applied, because this is already done by the methods themselves.

Algorithms for DiNA

We compared the performance of 10 different DiNA methods regarding their ability to recover key players in the cancer-specific GRNs* (including miRNA) to the performance in the corresponding GRNs. Each algorithm was applied only on the largest connected component of the networks. Here, we briefly describe each algorithm we considered. They all have in common that they (1) derive, for each network, a score per node (miRNA, TF or gene) and (2) compute a final ranking of nodes based on the differences in scores between the two networks (cancerous and control). In the following, v, u are nodes, A,B are the cancerous and control tissue networks, $d^X(v)$ is the degree of node v in network X and $c^X(u,v)$ is the correlation strength between nodes u and v, which is transformed to edge weights $w^X(u,v)$ in a particular way by each algorithm.

Differential Degree Centrality (DDC) [5]

DDC simply takes the normalized difference between a node's degrees in two networks. Degrees are normalized by the maximum degree in each network:

$$DDC(v) = \left|\frac{d^A(v)}{max_{u\in A}(d^A(u))} - \frac{d^B(v)}{max_{u\in B}(d^B(u))}\right|$$

DiffK algorithm [23]

The DiffK algorithm is based on DDC but considers edge weights. DiffK defines the score of a node v in network X as the sum of its edge weights:

$S^X_{DiffK}(v) = \sum_{u\in X} w^X(u,v)$ with $w^X(u,v) = |c^X(u,v)|$

DiffK(v) for a node v is then the absolute difference of the normalized scores in the two networks:

$$DiffK(v) = \left|\frac{S^A_{DiffK}(v)}{max_{u\in A}(S^A_{DiffK}(u))} - \frac{S^B_{DiffK}(v)}{maxu \in B(S^B_{DiffK}(u))}\right|$$

LS Measure [28]

The *LS* (v) of a node v is a variation of the DiffK algorithm, where scores are not normalized and the squared difference between adjacent edge weights is used:

$LS(v) = \sum_{u\in A|B} |w^A(u,v) - w^B(u,v)|^2$, with $w^X(u,v) = c^X(u,v)$

Odibat et al. [28] used the *LS* measure as a baseline for evaluating their DiffRank algorithm.

Differential DBC/DPC/DEC [13,28,34,35].

Several works proposed to use DPC centrality to study the role of nodes within a disease network and differential DPC centrality to find changes between two disease networks [28]. The DPC of a node v is the difference between its DPC scores $S^X_{PR}(v)$ in the two networks. Here, we also normalize the raw scores by the maximum score in the given network:

$DPC(v) = \left|\frac{S^A_{PR}(v)}{max_{u\in A}(S^A_{PR}(u))} - \frac{S^B_{PR}(v)}{max_{u\in A}(S^A_{PR}(u))}\right|$, with $w^X(u,v) = |c^X(u,v)|$

In the same way, we rank nodes using DBC centrality which considers shortest paths between all nodes of a network to calculate a score for node v. For calculating the shortest paths in single networks, weights are set to $w^X(u,v) = 1 - |c^X(u,v)|$ as stronger related nodes need a smaller edge weight to get a high betweenness score. For DEC, we rank the nodes in the same way with edge weights $w^X(u,v) = |c^X(u,v)|$.

DCLoc and DCGlob [21]

Bockmayr et al. developed two algorithms to identify differentially co-expressed nodes between two co-expression networks. The first algorithm, called DCLoc, compares the local topology of two networks, while the second, called DCGlob, compares global topologies. In a first step, the cancer-specific networks are constructed as described in the previous section but no significance threshold is applied. Next, the differential co-expression of each node is calculated as global topological change (comparison of connected components of the network) or local topological change (comparison of next neighbors of the investigated node) between the networks. The main characteristic of both algorithms is the repetition of this analysis for a series of 200 correlation thresholds, instead of using a single threshold. Results are averaged and a list of differentially correlated genes is obtained. For more details, see [21]. We slightly adapted both algorithms for regulatory networks. In regulatory networks, each node has much less edges than in a co-expression network. Therefore, in step 3 of the DCGlob algorithm, we lowered the expected cardinality of genes to 2 instead of 3. In step 2 of the DCLoc algorithm, we lowered the expected size of correlation clusters from 3 to 2.

DiffRank algorithm [28]

The DiffRank algorithm iteratively optimizes an objective function that is a linear combination of differential connectivity and DBC centrality within a DPC-style framework. Differential connectivity considers the difference in edge weights between two networks for a node v and the DiffRank scores of its neighbors. DFC centrality for a node v considers the difference in shortest paths that pass through v from s to t (with $s, t \neq v$) in network A versus network B and then sums all these absolute differences for all s, t. Note that this definition is different from the definition for DBC.

The algorithm combines both local and global properties into a single score. See [28] for details.

Differential motif centrality [36,34]

Motif centrality [36] calculates a score for each node in a network based on the number of certain motifs (here feed-forward loops (FFL)) the node is involved in. We extended this approach to also take edge weights into account (see Supplementary material S7.12). To compute DMC, we use the difference between the motif centrality scores in the two networks.

Gold standards for evaluation of DiNA algorithms

DiNA algorithms compute ranked list of nodes, reflecting the strength of changes these nodes underwent between the two networks being compared. To assess the quality of these rankings, we used GSLs.

For building the GSLs, we used the list of 138 cancer genes recently published by Vogelstein et al [37] extended by a list of cancer-specific miRNAs from the curated database mirCancer [69] (joint list henceforth called GSL_V). Genes and miRNAs not present in the GRN* after applying the correlation cutoff was removed, leading to different list sizes for the different cancer types (Table 6). TFs and genes from GSL_V were mapped to their corresponding HGNC symbol [65]. We also built cancer-type-specific GSLs using MalaCards (Version November 2015) [40] but as our experiences with these second GSLs were mixed, results regarding these GSLs are only covered in Supplementary S7.4. The performance of a DiNA algorithm with respect to any of these lists was obtained by computing the size of the intersection of the top-k nodes found by the algorithm with the respective (unranked) GSL. P values for the size of the overlaps for $k = 40$ were derived using Fishers exact test [70]. For selecting k, we took into account the distribution of differential centrality scores across the different DiNA algorithms and datasets. To consider only nodes whose differential centrality score is substantially higher than for most of the nodes, we visually chose a cutoff of $k = 40$ (Supplementary Figure S7.3). We used an absolute number for k rather than a percentage value for each network individually, as this would result in an unfair comparison, given the larger size of GRNs* compared with GRNs.

Clustering of DiNA methods

We were not only interested in the absolute performance of the different methods but also studied their inter-algorithm similarity by clustering them based on the overlap of their computed top-k lists using the Jaccard Index:

$$J(m_1, m_2, D) = \sum_{x\in D} \frac{1}{|D|} * \frac{|m_1(x) \cap m_2(x)|}{|m_1(x) \cup m_2(x)|}$$

Here, *m1* and *m2* are two DiNA methods, *D* contains the four cancer data sets and $|m_1(x) \cap m_2(x)|$ is the number of genes detected by m_1 and m_2 in data set *x*.

Randomization experiments

We performed two types of randomization experiments. First, we assigned random weights to all edges, leading to randomly weighted networks. Therefore, we started with GRN* for a specific cancer type and sampled correlation values from a normal distribution with mean and standard deviation equal to that of the original GRN*. Second, we shuffled the targets of all edges adjacent to a miRNA, leading to edge-shuffled networks. Here, we started with the GRN and added miRNAs using a random mapping to the nodes of the GRN* preserving the outdegree of all miRNAs. Edge weights for the randomized edges were randomly drawn from all correlation values assigned to edges with miRNAs in the GRN*. In each experiment, we generated 100 networks for each cancer type and corresponding control and computed the mean recovery rate within the top-40 entities for all DiNA algorithms.

Non-DiNA methods for comparison

We compared results from applying DiNA algorithms to two baselines. The first baseline ranks entities by their differential expression, disregarding any network structure. Differential expression was computed using *DESeq* [10], which uses an RNASeq-specific error model based on the negative binomial distribution. *P* values are multiple testing corrected using Benjamini–Hochberg [71]. All mRNAs and miRNAs with an adjusted *P* value $<= 0.05$ and a $\text{Log}_2\text{Fold} >= 1.5$ were ranked by their absolute Log_2Fold. We filtered for mRNAs and miRNAs present in the respective cancer or control GRNs* and selected the top-40.

The second baseline performs discriminative analysis based on a feature selection approach. We applied the MRMR method suggested by Ding and Peng [41]. As recommended by the authors, we discretized the data to three categorical states. We assume each gene expression to be negatively binomially distributed and used the $0.5 \pm k_x$-quantiles with $x \in \{miRNA, mRNA\}$ as thresholds. Best results were obtained using $k_{miRNA} = 0.3$ and $k_{mRNA} = 0.45$ for miRNA and mRNA data, respectively. We filtered for mRNAs and miRNAs present in the respective cancer or control GRNs* and selected the top-40 ranked mRNAs and miRNAs as most discriminative between cancer and control.

Key Points

- We compared the performance of 10 DiNA algorithms on four cancer transcriptome data sets for networks without miRNA to the performance for networks including miRNA using GSLs.
- Our results are a strong evidence for the strength of DiNA algorithms to find key players in regulatory networks based on transcriptome data.
- Consideration of miRNAs improves recovery rates for most tested algorithms.
- The evaluation of such algorithms is difficult, because no gold standard lists with a robust community acceptance exists and DiNA algorithms in general are very sensitive to the topology of the underlying networks.

Supplementary data

Supplementary data are available online at http://bib.oxfordjournals.org/.

Funding

This work was partly supported by the German Research Foundation [TRR54/1-2009]; and the German Federal Ministry of Education and Research [0316047B].

References

1. Schadt EE. Molecular networks as sensors and drivers of common human diseases. *Nature* 2009;**461**(7261):218–23.
2. Apic G, Ignjatovic T, Boyer S, *et al*. Illuminating drug discovery with biological pathways. *FEBS Lett* 2005;**579**(8):1872–7. PMID: 15763566.
3. Ideker T, Sharan R. Protein networks in disease. *Genome Res* 2008;**18**(4):644–52.
4. Pawson T, Linding R. Network medicine. *{FEBS} Lett* 2008;**582**(8):1266–70. (1) The Digital, Democratic Age of Scientific Abstracts (2) Targeting and Tinkering with Interaction Networks.
5. de la Fuente A. From 'differential expression' to 'differential networking' – identification of dysfunctional regulatory networks in diseases. *Trends Genet: TIG* 2010;**26**(7):326–33. PMID: 20570387.
6. Ideker T, Krogan NJ. Differential network biology. *Mol Syst Biol* 2012;**8**(1):565.
7. Cho D-Y, Kim Y-Ah, Przytycka TM. Chapter 5: network biology approach to complex diseases. *PLoS Comput Biol* 2012;**8**(12):e1002820.
8. Carulli JP, Artinger M, Swain PM, *et al*. High throughput analysis of differential gene expression. *J Cell Biochem* 1998; **72**(S30-31):286–96.
9. Wesley Hatfield G, Hung S-P, Baldi P. Differential analysis of DNA microarray gene expression data. *Mol Microbiol* 2003; **47**(4):871–7.
10. Anders S, Huber W. Differential expression analysis for sequence count data. *Genome Biol* 2010;**11**(10):R106. PMID: 20979621 PMCID: 3218662.
11. Trapnell C, Hendrickson DG, Sauvageau M, *et al*. Differential analysis of gene regulation at transcript resolution with RNA-seq. *Nat Biotechnol* 2013;**31**(1):46–53.
12. Joy MP, Brock A, Ingber DE, *et al*. High-betweenness proteins in the yeast protein interaction network. *J Biomed Biotechnol* 2005;**2005**(2):96–103. PMID: 16046814 PMCID: PMC1184047.
13. Wang H, Li M, Wang J, *et al*. *A New Method for Identifying Essential Proteins Based on Edge Clustering Coefficient*, Vol. **6674**. Berlin, Heidelberg: Springer, 2011, 87–98.
14. Li M, Wang J, Wang H, *et al*. *Essential Proteins Discovery from Weighted Protein Interaction Networks*, Vol. **6053**. Berlin, Heidelberg: Springer, 2010, 89–100.
15. Kim W, Li M, Wang J, *et al*. *Essential Protein Discovery Based on Network Motif and Gene Ontology*. Berlin, Heidelberg: Springer, 2011, 470–5.
16. Jaeger S, Ertaylan G, van Dijk D, *et al*. Inference of surface membrane factors of HIV-1 infection through functional interaction networks. *PLoS One* 2010;**5**(10):e13139.
17. Winter C, Kristiansen G, Kersting S, *et al*. Google goes cancer: improving outcome prediction for cancer patients by network-based ranking of marker genes. *PLoS Comput Biol* 2012;**8**(5):e1002511.

18. Bandyopadhyay S, Mehta M, Kuo D, *et al*. Rewiring of genetic networks in response to DNA damage. *Science (New York, NY)* 2010;**330**(6009):1385–9.
19. del Sol A, Balling R, Hood L, *et al*. Diseases as network perturbations. *Curr Opin Biotechnol* 2010;**21**(4):566–71.
20. Fukushima A. Diffcorr: an r package to analyze and visualize differential correlations in biological networks. *Gene* 2013;**518**(1):209–14. Proceedings of the 23rd International Conference on Genome Informatics (GIW 2012).
21. Bockmayr M, Klauschen F, Györffy B, *et al*. New network topology approaches reveal differential correlation patterns in breast cancer. *BMC Syst Biol* 2013;**7**(1):78.
22. Hudson NJ, Reverter A, Dalrymple BP. A differential wiring analysis of expression data correctly identifies the gene containing the causal mutation. *PLoS Comput Biol* 2009;**5**(5): e1000382.
23. Fuller TF, Ghazalpour A, Aten JE, *et al*. Weighted gene coexpression network analysis strategies applied to mouse weight. *Mamm Genome 2007*;**18**(6–7):463–72, 2007.
24. Carter SL, Brechbühler CM, Griffin M, *et al*. Gene co-expression network topology provides a framework for molecular characterization of cellular state. *Bioinformatics (Oxford, England)* 2004;**20**(14):2242–50.
25. Lai Y, Wu B, Chen L, *et al*. A statistical method for identifying differential gene-gene co-expression patterns. *Bioinformatics (Oxford, England)* 2004;**20**(17):3146–55.
26. Choi JK, Yu U, Yoo OJ, *et al*. Differential coexpression analysis using microarray data and its application to human cancer. *Bioinformatics* 2005;**21**(24):4348–55.
27. Huashan Y, Xiaowen L, Meng L, *et al*. MicroRNA and transcription factor co-regulatory network analysis reveals miR-19 inhibits CYLD in t-cell acute lymphoblastic leukemia. *Nucleic Acids Res* 2012;**40**(12):5201–14.
28. Odibat O, Reddy CK. Ranking differential genes in co-expression networks. *Proceedings of the 2nd ACM Conference on Bioinformatics, Computational Biology and Biomedicine – BCB '11* 2011, 350–4.
29. Guo H, Ingolia NT, Weissman JS, *et al*. Mammalian microRNAs predominantly act to decrease target mRNA levels. *Nature* 2010;**466**(7308):835–40.
30. Rajewsky N. microRNA target predictions in animals. *Nat Genet* 2006;**38**:S8–S13.
31. Jiang Q, Wang Y, Hao Y, *et al*. miR2Disease: a manually curated database for microRNA deregulation in human disease. *Nucleic Acids Res* 2009;**37**(Database issue):D98–D104. PMID: 18927107 PMCID: PMC2686559.
32. Esquela-Kerscher A, Slack FJ. Oncomirs-microRNAs with a role in cancer. *Nat Rev Cancer* 2006;**6**(4):259–69.
33. Thomas P, Durek P, Solt I, *et al*. Computer-assisted curation of a human regulatory core network from the biological literature. *Bioinformatics* 2014;**31**(8):1258–66.
34. Koschtzki D, Schreiber F. Centrality analysis methods for biological networks and their application to gene regulatory networks. *Gene Regul Syst Biol* 2008;**2**:193–201. PMID: 19787083 PMCID: PMC2733090.
35. Newman M. *Networks*. Oxford: Oxford University Press, 2010.
36. Koschtzki D, Schwbbermeyer H, Schreiber F. Ranking of network elements based on functional substructures. *J Theor Biol* 2007;**248**(3):471–9. PMID: 17644116.
37. Vogelstein B, Papadopoulos N, Velculescu VE, *et al*. Cancer genome landscapes. *Science* 2013;**339**(6127):1546–58.
38. Zhang H-M, Kuang S, Xiong X, *et al*. Transcription factor and microrna co-regulatory loops: important regulatory motifs in biological processes and diseases. *Brief Bioinformatics* 2015; **16**(1):45–58.
39. Schmeier S, Schaefer U, Essack M, *et al*. Network analysis of microRNAs and their regulation in human ovarian cancer. *BMC Syst Biol* 2011;**5**:183. PMID: 22050994 PMCID: 3219655.
40. Rappaport N, Nativ N, Stelzer G, *et al*. MalaCards: an integrated compendium for diseases and their annotation. *Database: J Biol Databases Curation* 2013;2013. PMID: 23584832 PMCID: PMC3625956.
41. Ding C, Peng H. Minimum redundancy feature selection from microarray gene expression data. *J Bioinformatics Comput Biol* 2005;**03**(02):185–205.
42. Schramm G, Kannabiran N, Konig R. Regulation patterns in signaling networks of cancer. *BMC Syst Biol* 2010;**4**(1):162.
43. Tsang J, Zhu J, van Oudenaarden A. MicroRNA-mediated feedback and feedforward loops are recurrent network motifs in mammals. *Mol Cell* 2007;**26**(5):753–67. PMID: 17560377 PMCID: PMC2072999.
44. Su W-L, Kleinhanz RR, Schadt EE. Characterizing the role of miRNAs within gene regulatory networks using integrative genomics techniques. *Mol Syst Biol* 2011;**7**:490. PMID: 21613979 PMCID: PMC3130556.
45. Friedman J, Alm EJ. Inferring correlation networks from genomic survey data. *PLoS Comput Biol* 2012;**8**(9):e1002687.
46. Lim WK, Wang K, Lefebvre C, *et al*. Comparative analysis of microarray normalization procedures: effects on reverse engineering gene networks. *Bioinformatics* 2007;**23**(13):i282–8.
47. Langfelder P, Horvath S. Wgcna: an r package for weighted correlation network analysis. *BMC Bioinformatics* 2008; **9**(1):559.
48. Cheng C, Yan K-K, Hwang W, *et al*. Construction and analysis of an integrated regulatory network derived from high-throughput sequencing data. *PLoS Comput Biol* 2011;**7**(11). PMID: 22125477 PMCID: 3219617.
49. Poos K, Smida J, Nathrath M, *et al*. How MicroRNA and transcription factor co-regulatory networks affect osteosarcoma cell proliferation. *PLoS Comput Biol* 2013;**9**(8):e1003210.
50. The cancer genome atlas. http://cancergenome.nih.gov, 2013.
51. R Development Core Team. R: A language and environment for statistical computing, 2005.
52. van Rossum G, Drake FL. Python reference manual, 2001.
53. Hagberg A, Swart P, Chult DS. Exploring network structure, dynamics, and function using networks. Technical Report LA-UR-08-05495; LA-UR-08-5495, Los Alamos National Laboratory (LANL), 2008.
54. Hsu S-D, Lin F-M, Wu W-Y, *et al*. miRTarBase: a database curates experimentally validated microRNAtarget interactions. *Nucleic Acids Res* 2011;**39**(Database issue):D163–9. PMID: 21071411 PMCID: PMC3013699.
55. Lewis BP, Burge CB, Bartel DP. Conserved seed pairing, often flanked by adenosines, indicates that thousands of human genes are MicroRNA targets. *Cell* 2005;**120**(1):15–20.
56. Wang X. mirdb: a microrna target prediction and functional annotation database with a wiki interface. *RNA* 2008;**14**(6): 1012–7.
57. John B, Enright AJ, Aravin A, *et al*. Human MicroRNA targets. *PLoS Biol* 2004;**2**(11). PMID: 15502875 PMCID: PMC521178.
58. Paraskevopoulou MD, Georgakilas G, Kostoulas N, *et al*. Diana-microt web server v5. 0: service integration into mirna functional analysis workflows. *Nucleic Acids Res* 2013;**41**(Web Server issue):W169–73.
59. Sethupathy P, Megraw M, Hatzigeorgiou AG. A guide through present computational approaches for the identification of mammalian microRNA targets. *Nat Methods* 2006;**3**(11):881–6.

60. Peterson SM, Thompson JA, Ufkin ML, *et al*. Common features of microrna target prediction tools. *Front Genet* 2014;**5**(23).
61. Matys V, Kel-Margoulies V. TRANSFAC and its module TRANSCompel: transcriptional gene regulation in eukaryotes. *Nucleic Acids Res* 2005;**34**.
62. Griffith OL, Montgomery SB, Bernier B, *et al*. ORegAnno: an open-access community-driven resource for regulatory annotation. *Nucleic Acids Res* 2008;**36**(Database issue):D107–13. PMID: 18006570 PMCID: PMC2239002.
63. Kolchanov NA, Podkolodnaya OA, Ananko EA, *et al*. Transcription regulatory regions database (TRRD): its status in 2000. *Nucleic Acids Res* 2000;**28**(1):298–301. PMID: 10592253.
64. Wang J, Lu M, Qiu C, *et al*. TransmiR: a transcription factor microRNA regulation database. *Nucleic Acids Res* 2010; **38**(Database issue):D119–22, PMID: 19786497 PMCID: 2808874.
65. Gray KA, Yates B, Seal RL, *et al*. Genenames. org: the hgnc resources in 2015. *Nucleic Acids Res* 2014;**42**:D749–D755.
66. Hauke J, Kossowski T. Comparison of values of pearson's and spearman's correlation coefficients on the same sets of data. *Quaestiones Geographicae* 2011;**30**(2):87–93.
67. Johnson P. Statistics for research, third edition. *Stat Methods Med Res* 2007;**16**(1):66–7.
68. Shapiro SS, Wilk MB. An analysis of variance test for normality (complete samples). *Biometrika* 1965;**52**:591–611.
69. Xie B, Ding Q, Han H, *et al*. miRCancer: a microRNAcancer association database constructed by text mining on literature. *Bioinformatics* 2013;**29**(5):638–44.
70. Fisher RA. On the interpretation of chi-square from contingency tables, and the calculation of p. *J R Stat Soc* 1922;**85**(1):87–94. ArticleType: research-article/Full publication date: Jan., 1922/Copyright 1922 Royal Statistical Society.
71. Benjamini Y, Hochberg Y. Controlling the false discovery rate: a practical and powerful approach to multiple testing. *J R Stat Soc. Ser B (Methodol)* 1995;**57**(1):289–300. ArticleType: research-article/Full publication date: 1995/Copyright 1995 Royal Statistical Society.